Progress of Theoretical Physics, Vol. 109, No. 5, May 2003

Upper Limit on the Mass of RX J1856.5–3754 as a Possible Quark Star

Kazunori KOHRI,[1] Kei IIDA[2] and Katsuhiko SATO[1,3]

[1]*Research Center for the Early Universe (RESCEU), School of Science, University of Tokyo, Tokyo 113-0033, Japan*
[2]*The Institute of Physical and Chemical Research (RIKEN), Wako 351-0198, Japan*
[3]*Department of Physics, School of Science, University of Tokyo, Tokyo 113-0033, Japan*

(Received October 11, 2002)

Recent deep Chandra LETG+HRC-S observations suggest the possibility that RX J1856.5–3754 is a compact star whose radiation radius is 3.8–8.2 km. In this paper, we systematically calculate the mass-radius relations of quark stars within the bag model. Assuming that RX J1856.5–3754 is a pure quark star, we derive an upper limit on its mass for various sets of bag-model parameters.

§1. Introduction

The possibility that compact stars supported by the degenerate pressure of quark matter exist has been investigated by many authors (see, e.g., Refs. 1) – 20)). The most commonly accepted picture of such quark stars is that a star containing quark matter in its core region, surrounded by hadronic matter, might exist in the branch of neutron stars;[13] this hypothesized type of star is often referred to as a "hybrid star". If hadronic matter in neutron stars can undergo a strong first-order phase transition, it is possible that a third family of more compact stars exists.[21] Such a third family, arising from a deconfinement phase transition, is predicted by a very restricted class of models of quark and hadronic matter.[14),15] As suggested by Witten,[10] there is another possible form of quark stars: If the true ground state of hadrons is "strange matter", bulk quark matter consisting of approximately equal numbers of u, d, and s quarks, then self-bound quark stars (or "strange stars") could occur at masses and radii on the order of or even smaller than those of typical neutron star, ~ 10 km and $\sim 1.4 M_\odot$. In the absence of reliable information about the equilibrium properties of hadronic and quark matter at high densities, however, it is impossible to tell which kind of quark stars is favored.

Recently, Drake et al.[22] reported that the deep Chandra LETG+HRC-S observations of the soft X-ray source RX J1856.5–3754 reveal an X-ray spectrum quite close to that of a blackbody of temperature $T = 61.2 \pm 1.0$ eV, and the data contain evidence for neither spectral features nor pulsation.*) They argued that the derived

*) They placed a 99% confidence upper limit of 2.7% on the unaccelerated pulse fraction from 10^{-4} to 100 Hz. Burwitz et al.[25] reported that a subsequent observation of RX J1856.5–3754 with *XMM-Newton* allows the upper limit on the periodic variation in the X-ray region to be reduced to 1.3% at 99% C.L. from 10^{-3} to 50 Hz.

interstellar medium neutral hydrogen column density is $N_H = (0.8\text{–}1.1) \times 10^{20}$ cm^{-2}, which, together with the results of recent HST parallax analyses, yields an estimate of 111–170 pc for the distance D to RX J1856.5–3754. Combining this range of D with the blackbody fit leads to a radiation radius of $R_\infty = 3.8\text{–}8.2$ km, which is smaller than typical neutron star radii and thus suggests that the X-ray source may be a quark star.

In a subsequent work, Walter and Lattimer [23] showed that the blackbody model of Drake et al. does not reproduce the observed UV/optical spectrum. [24] They succeeded in fitting the two-temperature blackbody and heavy-element atmosphere models developed in Ref. 24) to the observed spectrum, ranging from X-ray to optical wavelengths. They found that the radiation radius inferred from such a fitting lies between 12 km and 26 km, which is consistent with that of a neutron star. However, this model is not effective for explaining the lack of spectral features. Most recently, Braje and Romani [26] suggested that a two-temperature blackbody model, which can reproduce both the X-ray and optical-UV spectral data but seems to be inconsistent with the fact that pulsation is not detected, is indeed compatible with the interpretation that the object is a young normal pulsar, whose nonthermal radio beam misses Earth's line of sight. However, this model cannot answer why there are no features in the observed X-ray spectrum. In the absence of a model that accounts for all the observational facts, in this paper we employ the simple picture of Drake et al. [22] based on the uniform temperature blackbody fit to the X-ray spectrum.

From the radiation radius of RX J1856.5–3754 inferred from the blackbody fit to the X-ray spectrum, the upper bound of the star's mass can be derived. [27)–29)] This is because the radiation radius is larger than the true radius by a factor arising from gravitational redshift effects. The analysis of Drake et al. yields an upper bound of $0.5\text{–}1.1 M_\odot$. In previous studies, [27),29)] the mass-radius relations of pure quark stars were calculated from several kinds of equations of state (EOS) for quark matter, and these results were compared with the constraints on the mass and radius of RX J1856.5–3754 derived from the inferred radiation radius. In this framework, details of the relation between the mass of RX J1856.5–3754 and the EOS remains to be clarified. Further systematic investigations allowing for uncertainties in the EOS are needed; it is expected that these uncertainties can be reduced using Monte-Carlo calculations of lattice gauge theory at non-zero density, though such calculations at present are beset by technical problems.

Taking into account the above points in this paper, we consider the EOS of quark matter in the space of the parameters characterizing the bag model and investigate the question of how massive a quark star could be, given the inferred radiation radius. In §2, we construct quark stars using the bag-model EOS of quark matter. Section 3 is devoted to derivation of the mass-radius relation and its application to the soft X-ray source RX J1856.5–3754. Conclusions are given in §4. We use natural units in which $\hbar = c = k_{\rm B} = 1$ throughout the paper.

§2. Quark star models

To construct stars composed of zero-temperature *uds* quark matter, we start with the thermodynamic potentials, Ω_q, for a homogeneous gas of q quarks ($q = u, d, s$) of rest mass m_q to first order in α_c, where $\alpha_c \equiv g_c^2/4\pi$ is the fine structure constant associated with the QCD coupling constant g_c. In Refs. 30), 31) and 9), expressions for Ω_q are given as sums of the kinetic term and the one-gluon-exchange term at the renormalization scale $\Lambda = m_q$. We assume that $m_u = m_d = 0$ and write Ω_q as

$$\Omega_u = -\frac{{\mu_u}^4}{4\pi^2}\left(1 - \frac{2\alpha_c}{\pi}\right), \tag{2·1}$$

$$\Omega_d = -\frac{{\mu_d}^4}{4\pi^2}\left(1 - \frac{2\alpha_c}{\pi}\right), \tag{2·2}$$

$$\Omega_s = -\frac{m_s^4}{4\pi^2}\left\{x_s\eta_s^3 - \frac{3}{2}F(x_s) - \frac{2\alpha_c}{\pi}\left[3F(x_s)\left(F(x_s) + 2\ln x_s\right) - 2\eta_s^4 + 6\left(\ln\frac{\Lambda}{\mu_s}\right)F(x_s)\right]\right\}, \tag{2·3}$$

with

$$F(x_s) = x_s\eta_s - \ln\left(x_s + \eta_s\right), \tag{2·4}$$

where $x_s = \mu_s/m_s$, $\eta_s = \sqrt{x_s^2 - 1}$, μ_q is the chemical potential of q quarks, $\alpha_c = \alpha_c(\Lambda)$, and $m_s = m_s(\Lambda)$. In this paper we choose $\Lambda = \mu_s$.*)

In a star, electrons are distributed in such a manner that each local region is electrically neutral. (We ignore muons, which are more massive than electrons.) Since generally the electrons are dense enough to behave as an ultrarelativistic ideal gas, we can write the electron thermodynamic potential Ω_e in the massless noninteracting form,

$$\Omega_e = -\frac{{\mu_e}^4}{12\pi^2}, \tag{2·5}$$

where μ_e is the electron chemical potential.

In the bag model, we express the total energy density ρ as [32]

$$\rho = \sum_{i=u,d,s,e}\left(\Omega_i + \mu_i n_i\right) + B, \tag{2·6}$$

where B is the bag constant, i.e., the excess energy density effectively representing the nonperturbative color confining interactions, and n_i is the number density of i

*) Farhi and Jaffe [32] chose the renormalization scale as $\Lambda = 313$ MeV in describing self-bound *uds* quark matter in bulk; in such matter, the one-gluon-exchange interaction energy is small compared with the kinetic energy. Here we describe *uds* quark matter forming a system of stellar size, with a much wider density range. The present choice ($\Lambda = \mu_s$) is sufficient to keep the interaction energy relatively small for such a density range.

particles, given by

$$n_i = -\frac{\partial \Omega_i}{\partial \mu_i}. \tag{2·7}$$

Then, we obtain the pressure p as

$$\begin{aligned} p &= \mu_B n_B - \rho \\ &= -\sum_{i=u,d,s,e} \Omega_i - B, \end{aligned} \tag{2·8}$$

where $\mu_B = \sum_{i=u,d,s,e} n_i \mu_i / n_B$ is the baryon chemical potential, and

$$n_B \equiv \frac{1}{3}(n_u + n_d + n_s) \tag{2·9}$$

is the baryon density.

The values of the parameters m_s, α_c and B were obtained from fits to light hadron spectra in Refs. 33) – 35) (see Table I). However, the values yielded by such fits do not correspond to bulk quark matter.[32] Allowing for possible uncertainties, we consider values in the ranges $130 \leq B^{1/4} \leq 250$ MeV, $0 \leq m_s \leq 300$ MeV, and $0 \leq \alpha_c \leq 0.9$. The ranges of m_s and α_c so chosen are not consistent in all cases with the values in Table I, but they are consistent with the Particle Data Group[36] values renormalized at an energy scale of interest here.

To obtain the equilibrium composition of quark matter in its ground state at a given baryon density or chemical potential, the conditions of equilibrium with respect to the weak interaction and of overall charge neutrality must be imposed. These conditions are expressed by

$$\mu_u = \mu_d - \mu_e, \tag{2·10}$$

$$\mu_d = \mu_s, \tag{2·11}$$

and

$$\frac{2}{3} n_u - \frac{1}{3} n_d - \frac{1}{3} n_s = n_e. \tag{2·12}$$

From Eqs. (2·1)–(2·12), we can obtain the energy density and the pressure as functions of n_B (or μ_B).

In Figs. 1 and 2, we plot the energy per baryon (ρ/n_B) as a function of n_B^{-1}. We note that ρ/n_B becomes large as the strange quark mass m_s increases, because μ_s is an increasing function of m_s for fixed n_s. We also find that ρ/n_B increases as

Table I. Bag-model parameters fitted to hadron mass spectra.

$B^{1/4}$(MeV)	m_s (MeV)	α_c	Reference
145	279	2.2	T. DeGrand et al. (1975)[33]
200–220	288	0.8–0.9	C. E. Carlson et al. (1983)[34]
149	283	2.0	J. Bartelski et al. (1984)[35]

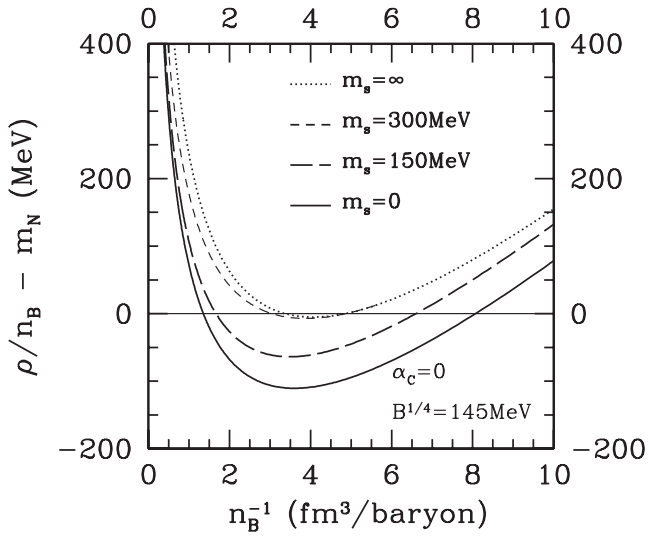

Fig. 1. Energy per baryon of electrically neutral quark matter in β equilibrium (minus the nucleon rest mass m_N) as a function of n_B^{-1}, calculated for $\alpha_c = 0$ and $B^{1/4} = 145$ MeV. The dotted curve is the result for ud quark matter ($m_s = \infty$). The dashed (long dashed) curve is the result for uds quark matter with $m_s = 300$ (150) MeV. The solid curve represents the result for a massless three-flavor system ($m_s = 0$).

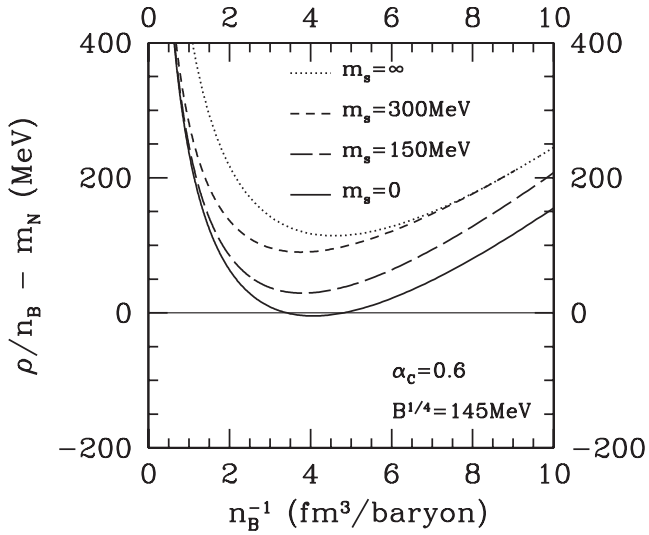

Fig. 2. Same as Fig. 1, but $\alpha_c = 0.6$.

α_c increases. This is because the one-gluon-exchange interaction is repulsive, due to the contribution from the exchange of transverse (magnetic) gluons in a relativistic quark plasma.

Figure 3 depicts the equation of state of ground-state quark matter, i.e., the pressure as a function of the energy density. From this figure, we see that the EOS becomes softer as B increases and hence as the color confining force increases. Such

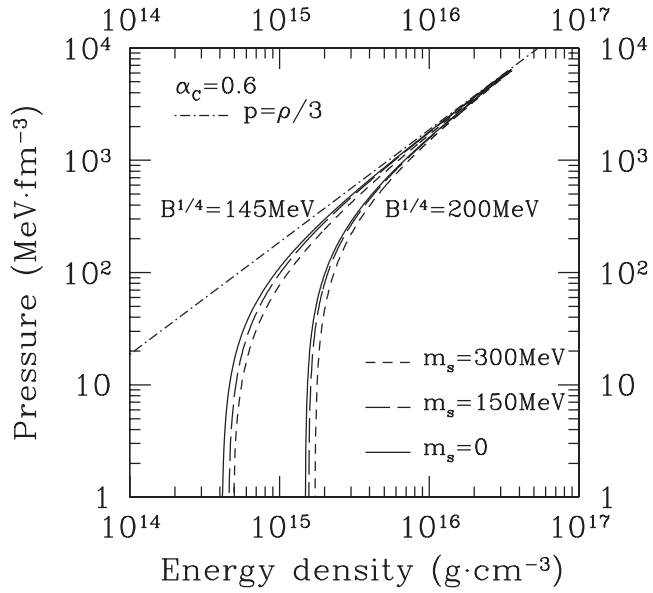

Fig. 3. Equation of state of *uds* quark matter in the ground state, calculated for $B^{1/4} = 145, 200$ MeV and $\alpha_c = 0.6$. The dashed, long dashed, and solid curves are the results for $m_s = 300, 150, 0$ MeV, respectively. The long dashed curve represents the EOS of a massless ideal gas ($p = \rho/3$).

a feature is explicitly expressed in Eq. (2·8). We also find that the EOS becomes softer as s quarks become more massive. This softening stems from the fact that a nonzero but small m_s acts to reduce the kinetic pressure of s quarks, as can be seen from Eq. (2·3). We remark in passing that as ρ increases the quark matter EOS becomes closer and closer to the massless ideal-gas limit ($p = \rho/3$).

We proceed to calculate the structure of nonrotating quark stars as in Refs. 11) and 12). Such calculations can be performed by incorporating the EOS models obtained above into the general relativistic equation of hydrostatic equilibrium, i.e., the Tolman-Oppenheimer-Volkoff (TOV) equation,[37]

$$\frac{dp(r)}{dr} = -G\frac{[\rho(r) + p(r)]\,[M(r) + 4\pi r^3 p(r)]}{r^2\left[1 - \dfrac{2GM(r)}{r}\right]}, \tag{2·13}$$

where G is the gravitational constant, r is the radial coordinate from the center of the star, and $M(r)$ is the gravitational mass of the stellar portion inside a surface of radius r, which can be obtained by integrating the equation for mass conservation,

$$\frac{dM(r)}{dr} = 4\pi r^2 \rho(r), \tag{2·14}$$

from 0 to r. Then, we can determine the radius, R, of the star from the condition that the pressure become zero, i.e., $p(r = R) = 0$. For various values of the energy density, ρ_0, at the center of the star, we finally obtain the radius R and the mass $M \equiv M(R)$.

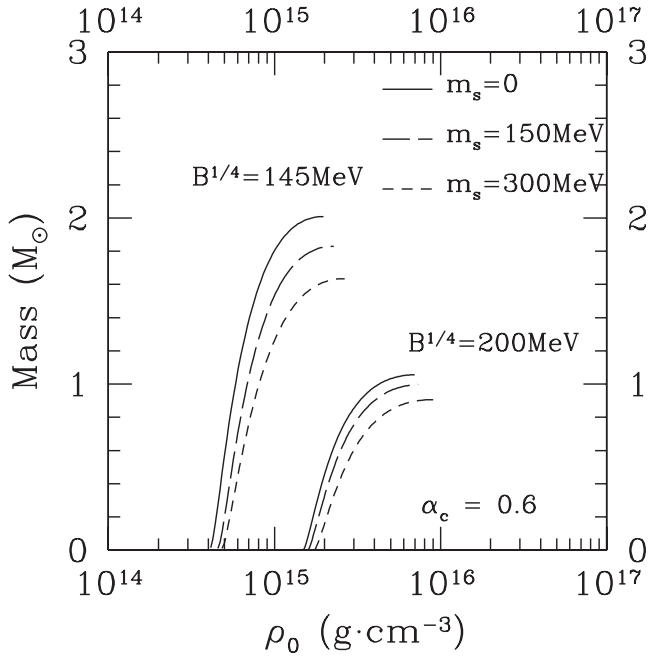

Fig. 4. Masses of pure quark stars with central energy density ρ_0, calculated for $B^{1/4} = 145, 200$ MeV and $\alpha_c = 0.6$. The dashed, long dashed, and solid curves are the results for $m_s = 300, 150, 0$ MeV, respectively.

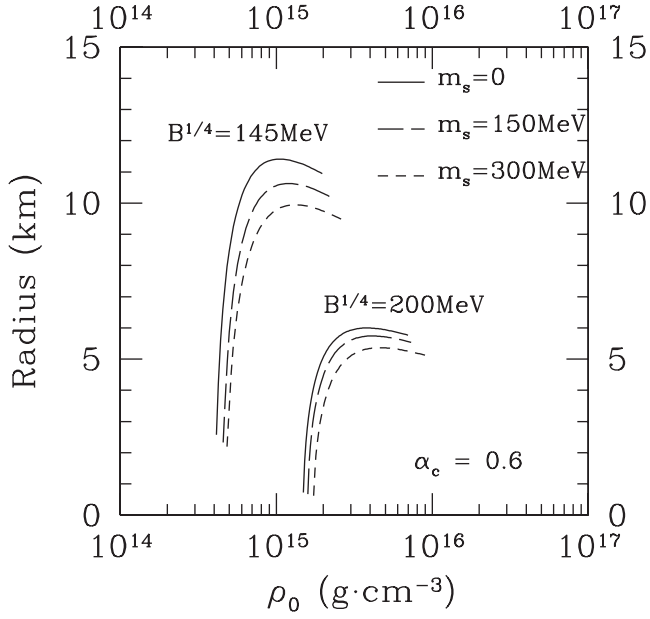

Fig. 5. Same as Fig. 4, except that the quantity plotted is the radius rather than the mass.

In Fig. 4 we plot the mass M as a function of ρ_0. In this figure, we include the M-ρ_0 relation up to the maximally allowed value of the mass; at this point, the star is no longer gravitationally stable.[38] We also exhibit the radius R as a function of ρ_0 in Fig. 5, where the right end of the R-ρ_0 relation corresponds to the maximum mass for a quark star.*) As can be seen in both Figs. 4 and 5, the radius and the mass become smaller for fixed ρ_0 as B and/or m_s increases, which leads to softening of the EOS (see Fig. 3). In other words, an increase in B and/or m_s for a fixed radius or mass tends to increase ρ_0.

§3. Upper limit on the mass of the possible quark star

In this section we derive the mass-radius relations of pure quark stars for various bag-model parameters and compare these relations with the inferred radiation radius of the soft X-ray source RX J1856.5–3754. We can straightforwardly calculate the mass-radius relations from the M-ρ_0 and R-ρ_0 relations obtained in the previous section. The results for $B^{1/4} = 145, 200$ MeV, $m_s = 0, 150, 300$ MeV, and $\alpha_c = 0.6$ are plotted in Figs. 6 and 7. The M-R relation ends at the maximum mass, where the gravitational instability sets in, while the mass M, when small, behaves as $\sim R^3$, due to the vacuum pressure B.

We now compare the obtained mass-radius relations of quark stars with the

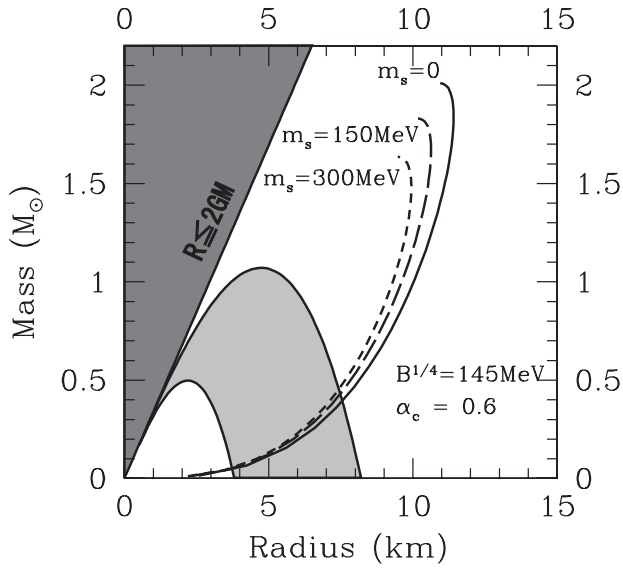

Fig. 6. Mass-radius relations of pure quark stars, calculated for $\alpha_c = 0.6$ and $B^{1/4} = 145$ MeV. The dashed, long dashed, and solid curves are the results for $m_s = 300, 150, 0$ MeV, respectively. The light shadowed region is allowed by the inferred radiation radius, $R_\infty = 3.8$–8.2 km, of RX J1856.5–3754. The dark shadowed region is excluded by the condition that R be larger than $2GM$.

*) For $m_s = 0$, the mass, radius and central energy density of a stable quark star of maximum mass are $M = 2.00 M_\odot (B_0/B)^{1/2}$, $R = 11.1$ km $(B_0/B)^{1/2}$ and $\rho_0 = 1.91 \times 10^{15}$ g cm^{-3} (B/B_0).[10]

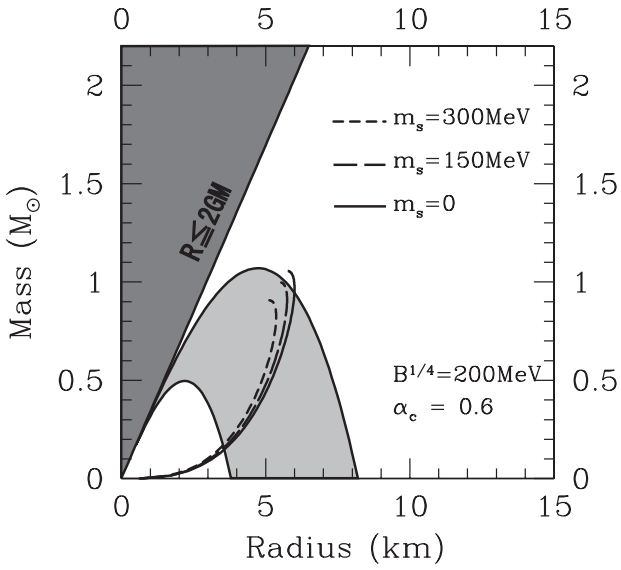

Fig. 7. Same as Fig. 6, but for $B^{1/4} = 200$ MeV.

inferred radiation radius of RX J1856.5–3754. According to the analysis of the deep Chandra LETG+HRC-S observation of RX J1856.5–3754 carried out by Drake et al.,[22] the X-ray spectrum is quite close to that of a blackbody of temperature $T = 61.2 \pm 1.0$ eV, and the X-ray luminosity is $L_X \simeq 6 \times 10^{31} (D/140 \text{ pc})^2 \text{ erg s}^{-1}$.[22] Then, we obtain the relation, $L_X = 4\pi R_\infty^2 (\pi^2/60T^4)$ between the luminosity and the temperature with the radiation radius R_∞ given by

$$R_\infty = \frac{R}{\sqrt{1 - \dfrac{2GM}{R}}}. \tag{3·1}$$

The factor $1/\sqrt{1 - 2GM/R}$ represents the redshift effect in a strong gravitational field. Drake et al.[22] inferred $R_\infty = 3.8$–8.2 km from the distance to RX J1856.5–3754, $D = 111$–170 pc.

Given such an inferred radiation radius R_∞, we can obtain information about the radius R and the mass M of the star from Eq. (3·1). In Figs. 6 and 7, the light shadowed region denotes the region of R and M allowed by the radiation radius $R_\infty = 3.8$–8.2 km. The dark shadowed region in these figures is excluded by the condition that the radius R of a radiation emitter be larger than a black hole surface of radius $2GM$. From these figures, we can see that the mass upper limit, $M_{\rm up}$, allowed by R_∞ increases from $\sim 0.4 M_\odot$ to $\sim 1 M_\odot$ when $B^{1/4}$ increases from 145 MeV to 200 MeV, while being almost independent of m_s. We remark that the mass lower limit allowed by R_∞ is of order $0.1 M_\odot$.

In Fig. 8 we plot the contours of the mass upper limit $M_{\rm up}$ in the space of the parameters $B^{1/4}$ and m_s, calculated for $\alpha_c = 0, 0.3, 0.6, 0.9$. From this figure, we find that the contours are peaked around $B^{1/4} \sim 200$ MeV. The left side of this peak results from the boundary of the allowed M-R region by the inferred radiation

radius of RX J1856.5–3754, while the right side is due to the maximum mass of gravitationally stable quark stars. We remark that for the smallest values of B, in addition to strange matter, even *ud* quark matter at zero pressure can be more stable than normal nuclei, as shown by Farhi and Jaffe.[32] We also note that the absolute stability of strange matter at zero pressure, which should allow for the existence of strange stars to exist, limits the bag-parameter region to the left side of the dot-dashed curves. It might be possible to relax this limitation if we consider that the bag constant depends on the pressure, as discussed in the Appendix.

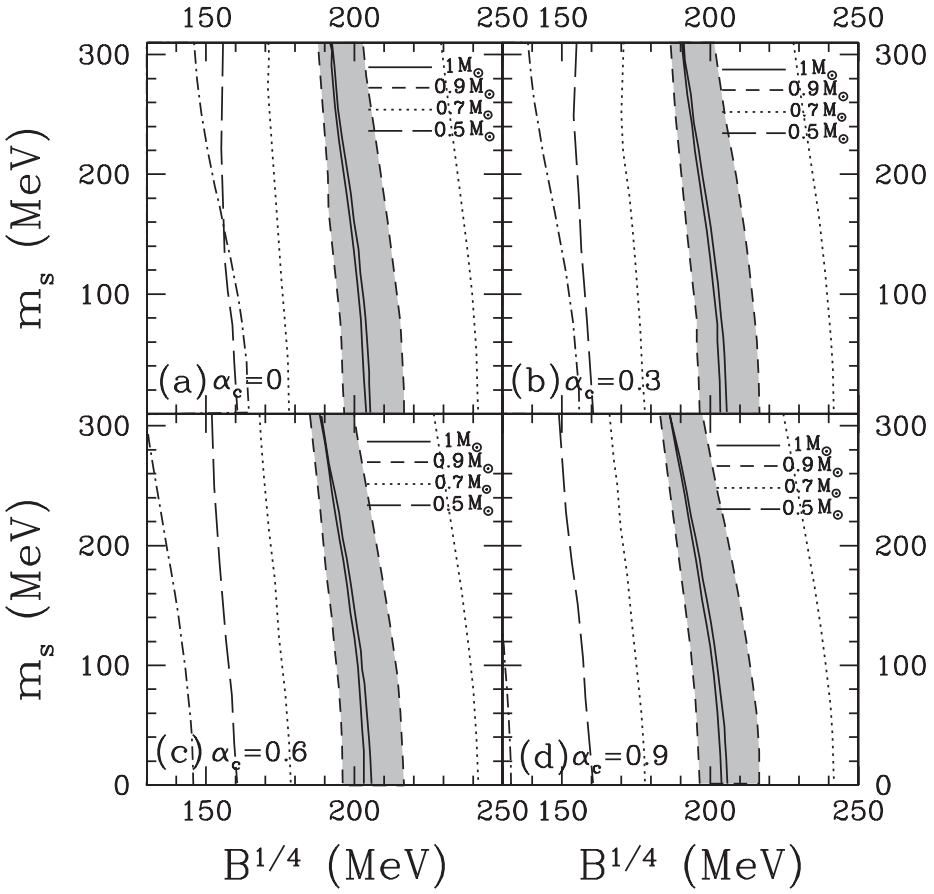

Fig. 8. Contours of the mass upper limit, $M_{\rm up}$, allowed by the inferred radiation radius of the soft X-ray source RX J1856.5–3754 in $B^{1/4}$–m_s plane, calculated for (a) α_c= 0, (b) 0.3, (c) 0.6, and (d) 0.9. In each panel the contours for $M_{\rm up} = 1M_\odot$ (solid curves), $M_{\rm up} = 0.9M_\odot$ (dashed curves), $M_{\rm up} = 0.7M_\odot$ (dotted curves), and $M_{\rm up} = 0.5M_\odot$ (long dashed curves) are included. For reference, we denote by the dot-dashed curves the boundary below which strange matter is absolutely stable at zero pressure (for details, see Fig. 1 in Farhi and Jaffe[32]).

§4. Conclusions

In this paper we have calculated the mass-radius relations of pure quark stars for various sets of bag-model parameter values. Assuming that RX J1856.5–3754 is a pure quark star, we have derived an upper limit on its mass, which is of order 0.5–1$M_\odot$. In such a star of $M \simeq 1M_\odot$, the central energy density would be $\sim 10^{16}$ g cm^{-3}. The present systematic analysis essentially includes the cases treated in previous analyses utilizing the EOS models based on perturbation theory [16),17)] and finite-temperature lattice data. [18)] Because this paper treats pure quark stars alone, however, many questions remain. We now discuss some of these.

Unless *uds* quark matter forms a more stable self-bound system than ^{56}Fe, a pure quark star would likely be unstable with respect to hadronization. The resultant star, no matter whether it be a hybrid star or a member of the third family mentioned in the Introduction, should have a larger radius for fixed central energy density with a hadronic shell surrounding a quark matter core. The extent to which the radius would increase depends strongly on the model of dense hadronic and quark matter used. Due to this increase, it is possible that the situation in which the bag-model parameter sets do not yield the absolute stability of *uds* quark matter would be in contradiction with the inferred radiation radius of RX J1856.5–3754, except for the case of possible parameter sets including large B for which the mass-radius relation of the third family enters the region allowed by the inferred radiation radius.

The possibility for the existence of a quark star of the third family depends on the condition that the velocity of sound be drastically enhanced at a deconfinement transition. [21)] It may be possible for this condition to be satisfied, as shown in Refs. 14) and 15) in the case in which the deconfinement transition is accompanied by a quark-hadron mixed phase including *uds* quark droplets embedded in a gas of electrons, in a sea of hadronic matter. This phase may be realizable because the presence of s and d quarks acts to reduce the electron Fermi energy and to enhance the proton fraction in hadronic matter. However, there are several reasons why it might be difficult for such a mixed phase to appear. First, the quark-hadron interfacial energy, which is poorly known, might be large enough to make the mixed phase energetically unfavorable. [39)] Second, even for fairly small values of the interfacial energy, electron screening of quark droplets could act to destabilize the mixed phase. [40)] Finally, even if the mixed phase is energetically favorable, it is uncertain how the mixed phase would nucleate in a neutron star. [41)]

If *uds* quark matter is absolutely stable, strange stars could exist, with a possible crust of nuclear matter. Such a crust would likely be composed of a Coulomb lattice of nuclei immersed in a roughly uniform gas of electrons, but not in a sea of neutrons. [11)] This nuclear matter including free neutrons would be surrounded by absolutely stable *uds* quark matter; the electric charge of the quark region, which is generally positive, would prevent the normal nuclei from contacting the quark matter. The effects of the crust on the strange star structure were investigated by Zdunik, [19)] He showed that the maximal presence of the crust would qualitatively change the mass-radius relation only for $M \lesssim 0.1M_\odot$. Determining to what extent the crust would prevail in a strange star requires information about the formation

and evolution of the star. We remark that even if RX J1856.5–3754 is a strange star, the surface of the star should be hadronic. This is because the observed spectrum is of blackbody type, while at the observed X-ray luminosity, the spectrum emitted from a bare quark matter surface would differ drastically from the blackbody spectrum.[42]

Information about the mass of RX J1856.5–3754 is useful to distinguish between the possible forms of compact stars. In order to derive a constraint on the mass from the observed X-ray luminosity L_X, it is instructive to note the possible origins of L_X. Initial cooling and accretion of interstellar material are generally considered to be responsible for L_X.[43] We may thus assume that the gravitational energy release of the accreting material is smaller than L_X, i.e., $L_X \gtrsim GM\dot{M}/R$, with the Bondi accretion rate $\dot{M}$ onto a star moving supersonically in an ambient medium given by[44]

$$\dot{M} = 4\pi\lambda \left(\frac{GM}{v^2}\right)^2 \rho_H v. \tag{4·1}$$

Here, λ is an $\mathcal{O}(1)$ constant related to the EOS of the accreting matter, v is the velocity of the star, and ρ_H is the hydrogen mass density ($= m_N n_H$ with nucleon mass m_N and hydrogen number density n_H). The velocity v has been determined as $v \simeq 200(D/140\ \mathrm{pc})\ \mathrm{km\ s^{-1}}$ from observations of the proper motion of the optical counterpart of RX J1856.5–3754.[23] In order to estimate n_H, we follow the argument of Ref. 28). The hydrogen number density is roughly given by $n_H = N_H/R_H$, where N_H is the column density to the star derived from the blackbody fit to the X-ray spectrum as $N_H = (0.8\text{–}1.1) \times 10^{20}\ \mathrm{cm^{-2}}$,[22] and R_H is the size of the local high density region. R_H could be on the order of 100 AU or even less, as is known from observations of the interstellar medium using the 21 cm HI line.[45] From Eq. (4·1), we can thus estimate the mass of the star as

$$M \lesssim 0.4M_\odot \left(\frac{v}{200\ \mathrm{km}}\right) \left(\frac{D}{140\ \mathrm{pc}}\right)^{5/3} \left(\frac{N_H}{10^{20}\ \mathrm{cm^{-2}}}\right)^{-1/3} \left(\frac{R_H}{100\ \mathrm{AU}}\right)^{1/3} \times \left(\frac{R}{5\ \mathrm{km}}\right)^{1/3}. \tag{4·2}$$

Uncertainties in Eq. (4·2) come mainly from the velocity v and the local high density scale R_H. The actual values of v and R_H depend on the poorly known radial velocity and density profile in the R CrA molecular cloud believed to contain RX J1856.5–3754. Therefore, M may in fact be much larger than $0.4M_\odot$. However, it is interesting to note that the mass range estimated from the X-ray luminosity L_X, which is almost independent of the spectral analysis leading to the allowed M-R region depicted in Figs. 6 and 7, may play a role in narrowing the allowed M-R region and hence in clarifying the composition of this compact star.

Elucidating the formation of quark stars is another important problem. If quark stars of masses smaller than $\sim 1M_\odot$ are converted from neutron stars with canonical masses of order $1.4M_\odot$, material in a neutron star should be partly ejected out of the star and partly changed into quark matter. Thus, possible scenarios for the

formation of low-mass quark stars (some of which are discussed in Refs. 46) and 28)) depend inevitably on the initial and final configuration of the stars.

Acknowledgements

K. K. wishes to thank Takashi Nakamura, T. Shigeyama, Shoichi Yamada, S. Nagataki, and G. Watanabe for useful discussions and comments. This work was supported in part by Grants-in-Aid for Scientific Research provided by the Ministry of Education, Culture, Sports, Science and Technology of Japan through Research Grant Nos. S14102004 and 14079202, and in part by RIKEN Special Postdoctoral Researchers Grant No. 011-52040.

Appendix A

—— Effects of the Pressure Dependent Bag Constant ——

In this appendix, we modify the bag model adopted in the main text by allowing the bag constant to depend on the pressure. In the model thus modified, it is possible for the bag constant inside the star to become effectively larger than that at the surface. Then, the absolute stability condition of strange matter at zero pressure, which is characterized by the dot-dashed curves in Fig. 8, can be changed significantly. In the main text, we studied the mass-radius relations of pure quark stars, with B fixed throughout the interiors, and extrapolated our calculations beyond the absolutely stable region. As we see below, however, the stable region can be enlarged by the pressure dependence of the bag constant.

As discussed in Refs. 18) and 20), we can generally parameterize the EOS of strange matter in the massless limit ($m_s \to 0$) as

$$p = \frac{1}{A}\left(\rho - 4B\right), \tag{A·1}$$

where A is a parameter, whose value is three in the standard bag model. Then, we can transform Eq. (A·1) into

$$p = \frac{1}{3}(\rho - 4B_{\rm eff}), \tag{A·2}$$

where $B_{\rm eff}$ is the effective bag constant, which depends on the pressure p (or the energy density ρ) as

$$\begin{aligned} B_{\rm eff} &\equiv \frac{1}{4}\left(A-3\right)p + B, \\ &= \frac{1}{4}\left(1 - \frac{3}{A}\right)\rho + \left(\frac{3}{A}\right)B. \end{aligned} \tag{A·3}$$

$B_{\rm eff}$ reduces to B in the limit $p \to 0$. From Eq. (A·3), we find that if A is larger than three, $B_{\rm eff}$ becomes larger than B inside the star. In the model used in Ref. 18), A takes a typical value of 3.8, while $A \approx 2.2$ in Ref. 20). Here we consider the range of values $A = 2$–6. We remark that there should be an upper bound on A; at non-zero

pressures, if A is far greater than unity, the effective bag constant is increased to such an extent that hadronic matter can be energetically favored even at extremely high pressures.

We now consider calculations of mass-radius relations of pure quark stars from the EOS (A·1). By repeating the calculations performed in §2 for $B_{\rm eff}$ rather than B, we can compute the central pressure of a stable quark star of maximum mass for various values of A and B. In Fig. 9, we plot the contours of the effective bag constant $B_{\rm eff}^{1/4}$ at this central pressure in the $B^{1/4}$–A plane. We denote by the dot-dashed curve the boundary of the region in which strange matter at the surface ($p = 0$) is absolutely stable ($B^{1/4} \leq 165$ MeV). From this figure, we see that at a critical value of $B^{1/4} = 165$ MeV, $B_{\rm eff}$ can be as large as 200 MeV inside the star for $A \gtrsim 4$. Since such large values of $B_{\rm eff}$ effectively soften the EOS of strange matter, the bag model with a pressure dependent bag constant allows for the possibility of strange stars that are more compact than those predicted by the bag model, as plotted in Fig. 6, for fixed B.

In order to see how the resultant softening of the strange matter EOS affects the upper limit of the mass, $M_{\rm up}$, allowed by the inferred radiation radius of the soft X-ray source RX J1856.5–3754, we plot the contours of $M_{\rm up}$ in the $B^{1/4}$–A plane (see Fig. 10). When $A > 3$, quark stars which are more massive than those allowed by the bag model prediction ($A = 3$) exist in the region of the absolute stability of strange

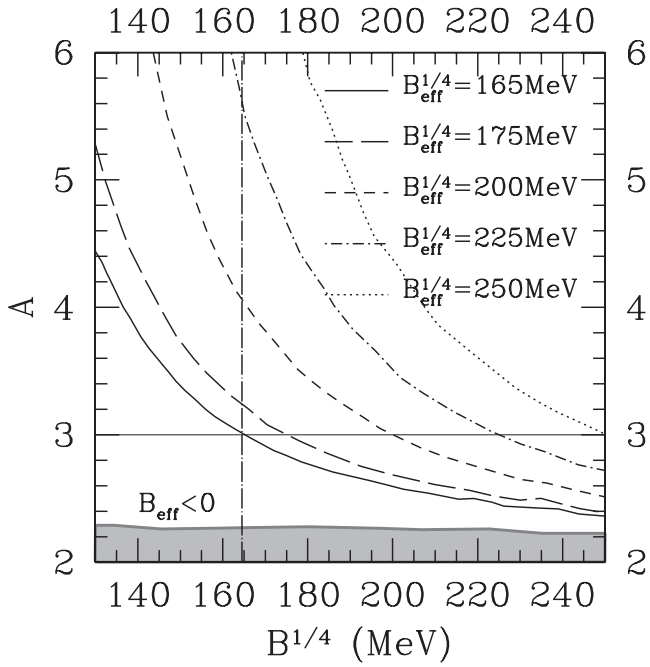

Fig. 9. Contours of the effective bag constant $B_{\rm eff}^{1/4}$ at the central pressure of a stable quark star of maximum mass in the $B^{1/4}$–A plane, calculated for $\alpha_c = 0$. The vertical dot-dashed curve is the boundary of the region in which strange matter is absolutely stable at zero pressure ($B^{1/4} \leq 165$ MeV). The shadowed region corresponds to $B_{\rm eff} \leq 0$.

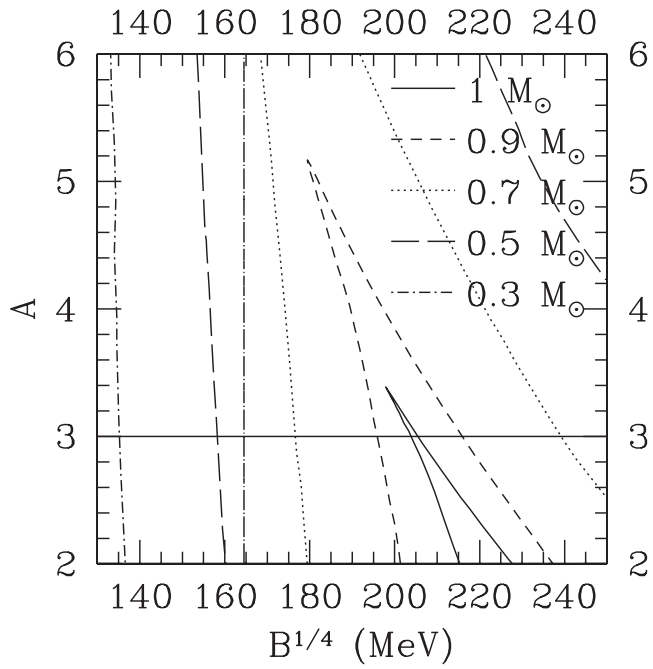

Fig. 10. Contours of the upper limit of the mass, $M_{\rm up}$, allowed by the inferred radiation radius of the soft X-ray source RX J1856.5–3754 in the $B^{1/4}$–A plane, calculated for $\alpha_c = 0$. The contours of $M_{\rm up} = 1M_\odot$ (solid curves), $M_{\rm up} = 0.9M_\odot$ (dashed curves), $M_{\rm up} = 0.7M_\odot$ (dotted curves), $M_{\rm up} = 0.5M_\odot$ (long dashed curves) and $M_{\rm up} = 0.3M_\odot$ (dot-short-dashed curves) are included. The vertical dot-dashed curve is the boundary of the region in which strange matter is absolutely stable at zero pressure ($B^{1/4} \leq 165$ MeV).

matter at zero pressure. Because the inferred radiation radius of RX J1856.5–3754 is very small, however, the change is small for $A \sim 4$.

References

1) D. Ivanenko and D. F. Kurdgelaidze, Lett. Nuovo Cim. **2** (1969), 13.
2) N. Itoh, Prog. Theor. Phys. **44** (1970), 291.
3) J. C. Collins and M. J. Perry, Phys. Rev. Lett. **34** (1975), 1353.
4) G. Baym and S. A. Chin, Phys. Lett. B **62** (1976), 241.
5) G. Chapline and M. Nauenberg, Nature **264** (1976), 235; Phys. Rev. D **16** (1977), 450.
6) M. B. Kislinger and P. D. Morley, Astrophys. J. **219** (1978), 1017.
7) W. B. Fechner and P. C. Joss, Nature **274** (1978), 347.
8) B. A. Freedman and L. D. McLerran, Phys. Rev. D **17** (1978), 1109.
9) V. Baluni, Phys. Lett. B **72** (1978), 381; Phys. Rev. D **17** (1978), 2092.
10) E. Witten, Phys. Rev. D **30** (1984), 272.
11) C. Alcock, E. Farhi and A. Olinto, Astrophys. J. **310** (1986), 261.
12) P. Haensel, J. L. Zdunik and R. Schaeffer, Astron. Astrophys. **160** (1986), 121.
13) A. Rosenhauer, E. F. Staubo, L. P. Csernai, T. Øvergård and E. Østgaard, Nucl. Phys. A **540** (1992), 630.
14) N. K. Glendenning and C. Kettner, Astron. Astrophys. **353** (2000), L9.
15) K. Schertler, C. Greiner, J. Schaffner-Bielich and M. H. Thoma, Nucl. Phys. A **677** (2000), 463.
16) E. S. Fraga, R. D. Pisarski and J. Schaffner-Bielich, Phys. Rev. D **63** (2001), 121702(R).
17) J. O. Andersen and M. Strickland, Phys. Rev. D **66** (2002), 105001.

18) A. Peshier, B. Kämpfer and G. Soff, hep-ph/0106090.
19) J. L. Zdunik, Astron. Astrophys. **394** (2002), 641.
20) M. Sinha, J. Dey, M. Dey, S. Ray and S. Bhowmick, Mod. Phys. Lett. A **17** (2002), 1783.
21) U. H. Gerlach, Phys. Rev. **172** (1968), 1325.
22) J. J. Drake et al., Astrophys. J. **572** (2002), 996.
23) F. M. Walter and J. M. Lattimer, Astrophys. J. **576** (2002), L145.
24) J. A. Pons, F. M. Walter, J. M. Lattimer, M. Prakash, R. Neuhäuser and P. An, Astrophys. J. **564** (2002), 981.
25) V. Burwitz, F. Haberl, R. Neuhaeuser, P. Predehl, J. Truemper and V. E. Zavlin, Astron. Astrophys. (in press), astro-ph/0211536.
26) T. M. Braje and R. W. Romani, Astrophys. J. **580** (2002), 1043.
27) A. R. Prasanna and S. Ray, astro-ph/0205343.
28) T. Nakamura, astro-ph/0205526.
29) D. Gondek-Rosinska, W. Kluzniak and N. Stergioulas, astro-ph/0206470.
30) G. Baym and S. A. Chin, Nucl. Phys. A **262** (1976), 527.
31) B. A. Freedman and L. D. McLerran, Phys. Rev. D **16** (1977), 1130; ibid. **16** (1977), 1147; ibid. **16** (1977), 1169.
32) E. Farhi and R. L. Jaffe, Phys. Rev. D **30** (1984), 2379.
33) T. DeGrand, R. L. Jaffe, K. Johnson and J. E. Kiskis, Phys. Rev. D **12** (1975), 2060.
34) C. E. Carlson, T. H. Hansson and C. Peterson, Phys. Rev. D **27** (1983), 1556.
35) J. Bartelski, A. Szymacha, Z. Ryzak, L. Mankiewicz and S. Tatur, Nucl. Phys. A **424** (1984), 484.
36) K. Hagiwara et al. [Particle Data Group Collaboration], Phys. Rev. D **66** (2002), 010001.
37) J. R. Oppenheimer and G. M. Volkoff, Phys. Rev. **55** (1939), 374.
38) S. L. Shapiro and S. A. Teukolsky, *Black Holes, White Dwarfs, and Neutron Stars* (Wiley, New York, 1983).
39) H. Heiselberg, C. J. Pethick and E. F. Staubo, Phys. Rev. Lett. **70** (1993), 1355.
40) D. N. Voskresensky, M. Yasuhira and T. Tatsumi, Phys. Lett. B **541** (2002), 93.
41) K. Iida and K. Sato, Prog. Theor. Phys. **98** (1997), 277; Phys. Rev. C **58** (1998), 2538.
42) D. Page and V. V. Usov, Phys. Rev. Lett. **89** (2002), 131101.
43) F. M. Walter, S. J. Wolk and R. Neuhäuser, Nature **379** (1996), 233.
44) H. Bondi and F. Hoyle, Mon. Not. R. Astron. Soc. **104** (1944), 273.
45) D. A. Frail et al., Astrophys. J. **436** (1994), 144.
46) R. Ouyed, J. Dey and M. Dey, Astron. Astrophys. **390** (2002), L39.